Int. J. Electrochem. Sci., 11 **(2016)** 3555 - 3566

International Journal of ELECTROCHEMICAL SCIENCE
www.electrochemsci.org

Synergistic Effects of Bismuth Adatoms on Electrocatalytic Properties of Electrodeposited Nanostructured Platinum Electrodes

Mohammed Khair Hourani[*] *and Ahmad Alkawaldeh*

Department of Chemistry, Electrochemistry Research Laboratory, University of Jordan, Amman 11942, Jordan
[*]E-mail: mhourani@ju.edu.jo, hourani.khair.2015@gmail.com

Received: 3 February 2016 / *Accepted:* 14 March 2016 / *Published:* 1 April 2016

An innovative simple procedure for preparation of platinum nanostructured electrode deposited on a tantalum substrate by application of a square wave potential regime has been established. The potential regime comprises a square wave between two limits, the lower limit allows spontaneous deposition of platinum while the upper limit does not. The dependence of the produced particles in terms of size and uniformity of distribution was explored. The optimal conditions for preparation of the nanostructured platinum deposits were 100 Hz frequency, -0.4 V and 0.00 V lower and higher limits of the square wave respectively with an amplitude of 0.4 V . The optimal concentration of $PtCl_4^-$ was $1.0x10^{-3}$ M. The prepared surfaces were allowed to contact 0.5 M H_2SO_4 + $1x10^{-3}$ M Bi^{3+} solution were Bi atoms were irreversibly adsorbed at the platinum nanostructured surfaces to form $Pt_{nano}Bi_{ad}$ surfaces (a notation for platinum nanostructured surface with irreversibly adsorbed Bi atoms). The electrocatalytic properties of $Pt_{nano}Bi_{ad}$ catalytic surfaces were tested for electrooxidation of methanol and formic acid. $Pt_{nano}Bi_{ad}$ electrode showed higher electrocatalytic properties than the plain Pt_{nano} electrode. This proves the notion of the synergistic effects of Bi adatoms and nanostructured surfaces in imparting higher electrocatalytic properties to platinum electrodes.

Keywords: platinum nanostructured electrodes, adatom electrodes, synergistic catalytic effects, electroxidation of methanol, electroxidation of formic acid.

1. INTRODUCTION

Nanostructured electrodes present a new chapter in surface electrochemistry[1]. The unique surface properties and the capability of chemical surface functionalization by adsorption or anchoring of chemical moieties at the nanostructured surfaces opens avenues of potential applications for these

doi: 10.20964/110434

surfaces[2] . Electrocatalysis, electroanalysis and energy conversion are among many fields which benefit from nanostructured electrodes[3,4,5]. Preparation of nanostructured surfaces by electrodeposition provides a competent route for preparation of nanostructured surfaces[6].

Adatoms on metallic surfaces, on the other hand, imitate inexpensive and reversibly made surface alloys[7]. Previous studies on adatom electrodes indicated that many metallic adatom electrodes have higher catalytic properties compared with their corresponding plain metallic electrodes[8,9]. Moreover, preparation of adatom surfaces involves a simple procedure which involves exposure of the metallic substrates to solutions containing ions of the adatoms under open-circuit or potentiostatic conditions[10] .

Many investigated adatom-substrate surfaces showed enhanced electrocatalytic properties towards many vital electrochemical processes such oxidation of small organic molecules which might be utilized in fuel cells [11]. On the premise that the combination of both, adatoms atop of nanostructured electrodes may provide superior surfaces in terms of electrocatalytic properties the present work was undertaken. The present wok aims at preparation of nanostructured platinum electrodes decorated with bismuth adatoms and investigation of their electrocatalytic properties towards electrooxidation of some organic test molecules.

2. EXPERIMENTAL

2.1. Instruments, cells, and electrodes

A potentiostat (PARC Model 273 A (EG & G) interfaced to a computer via GPIB interface along with Echem® software (PARC instruments, EG & G) was used for electronic control and data acquisition of the electrochemical experiments. The square wave with the preset amplitude and frequency was generated by a function generator (Simpson, A240). The desired lower and higher limits of the potential regime were obtained by adjusting the applied electrode potential from the potentiostat and or the voltage offset from the function generator. The square wave as applied to the electrode was monitored via an oscilloscope (Telequipment S540).

Two cells were used in pursuing the present work; an analytical cell for recording cyclic voltammograms to characterize the starting and prepared surfaces, and a deposition cell for deposition of nanoparticles on tantalum substrates. The analytical cell was a conventional, H-shape cell with two compartments , one for accommodation of the working electrode while the other for housing the reference and the auxiliary electrodes. The analytical cell was equipped with a multiple inlet/outlet system for admission of supporting electrolyte, deaeration and blanketing the solution with oxygen-free nitrogen. The working electrode was a 1.0 mm diameter tantalum electrode (99.9% pure, Goodfellow). The immersed part of the wire was curved in order to provide a mark for obtaining a reproducible surface area of the electrode. The reference electrode was an Ag/AgCl/ $[Cl^-]$ = 1.0 M, and all the potentials reported in this paper are referenced to this electrode. The auxiliary electrode was made of platinum (Johnson Matthy, 99.99% minimum purity) wire which was coiled into a spiral to provide a large surface area.

A modified Polarographic 303A cell (Princeton Applied Research) was used for electrodeposition of the metallic nanostructures. The cell was modified by bypassing the electronic circuitry of the 303 Polarographic Stand and using the three electrode cell system externally for the deposition process with Ag/AgCl, [Cl^-] = 1.0 M reference electrode. The deposited samples were viewed by scanning electron microscope (Inspect F50, FEI company, Netherlands). The electron microscope was coupled with an EDX electron microanalyzer which allowed investigation of the elemental composition of deposited structures.

2.2. Materials

All reagents used were highly pure certified analytical reagent (A.R.) chemicals, and were used as received from the suppliers without further purification. Hexachloroplatinate solution (1 mg platinum /ml) dissolved in 10% HCl was purchased from Janssen Chemicals, USA. Adatom solution was made from Bismuth (III) nitrate (Sigma-Aldrich, 98%, USA). Methanol (99.95%) was purchased from Sigma-Aldrich. Formic acid (98% pure was supplied by Sigma Aldrich. Sulfuric acid (97%) was purchased from Fluka, and nitric acid (69%) was supplied from Sharlu, Spain). The purging nitrogen was G5 grade (99.999% minimum purity) supplied by the National Gas Company and coupled with Oxisorb® cartridge (Supelco) to ensure effective removal of any traces of oxygen. All solutions were made from the above-mentioned reagents dissolved in Millipore water (Merck Millipore) of 18.2 MΩ and total dissolved solids less than 5 ppb. All experiments were carried out at ambient temperatures.

2.3 Procedures

Each experiment was commenced by chemical polishing of the substrate, a tantalum wire. The chemical polishing was achieved by immersion in a solution of 5:2:2 (v:v:v) 98% H_2SO_4, 65% HNO_3, and water followed by immersion in 48% HF. The chemically etched tantalum substrate was then extensively rinsed with Millipore water. The clean tantalum wire was mounted in the electrochemical cell. The measured rest potential was about -0.6 V. The electrode was cathodized at the above-mentioned rest potential for 5 min to ensure removal of any traces of oxide, if any, from the surface. The cyclic voltammograms of the oxidized and oxide-free tantalum surface are published elsewhere [12]. In all experiments the potential of the bare tantalum electrode was maintained below - 0.6 V to avoid oxidation of the tantalum surface and to ensure that the metallic nanostructured surfaces were developed on a clean, oxide-free tantalum surface.

Electrodeposition of platinum nanostructured surfaces on tantalum electrodes was carried out in 0.5 M H_2SO_4 + 1.0×10^{-3} M $PtCl_6^-$ solution. The solutions were stirred, purged and blanketed with oxygen-free nitrogen gas during the deposition period. Electrodeposition was induced from the above-mentioned solution by application of a square wave potential regime.. Deposition of platinum nanostructures by application of square wave potential regimes was optimized by variation of the experimental conditions. These included the characteristics of the square wave, the deposition time and the concentration of platinum salt. The concentration of the $PtCl_6^-$ was varied between $1.0x10^{-4}$ M

and $1.0x10^{-2}$ M while the deposition time was varied between 90, 120, and 180 s. The characteristics of the square wave involved variation of the frequency, the upper and lower limits, and the amplitude of the square wave. The size of the nanoparticles was estimated by measurement of the size of the particles on the SEM micrograph. The number of nanoparticles on the substrate surface was estimated by manual counting and averaging the number of particles in known areas on the SEM micrograph. Uniformity of distribution of nanoparticles on the surface was evaluated by visual inspection of the SEM micrographs. The prepared surfaces were judged in terms of size, number of the nanoparticles per square centimeter and uniformity of their distribution on the substrate surface

After preparation of the nanostructured platinum surfaces onto tantalum substrate, the electrode was rinsed extensively with Millipore water. The electrode was then allowed to contact a 0.5 M H_2SO_4 solution containing $1.0x10^{-3}$ M of Bi^{3+} ions. The nanostructured platinum surfaces modified with bismuth adatoms were characterized by cyclic voltammetry, SEM, EDX x-ray spectroscopy and voltammetry of Ag^+ electrodeposition as a surface-sensitive electrodeposition. The electrocatalytic properties of the modified surfaces were investigated by following there poteniodynamic curves in supporting electrolyte solutions containing test organic molecules such as methanol and formic acid. Chronoampermetric measurements were also conducted for investigation of the kinetics of HCOOH electrooxidation at the nanostructured platinum electrodes modified by bismuth adatoms. The experiments involved stepping the electrode potential from 0.15 V to 0.80 V for 0.70 s in the supporting electrolyte containing formic acid.

3. RESULTS AND DISCUSSION

3.1 The effect of $PtCl_6^-$ concentration and deposition time on the deposited platinum nanostructures

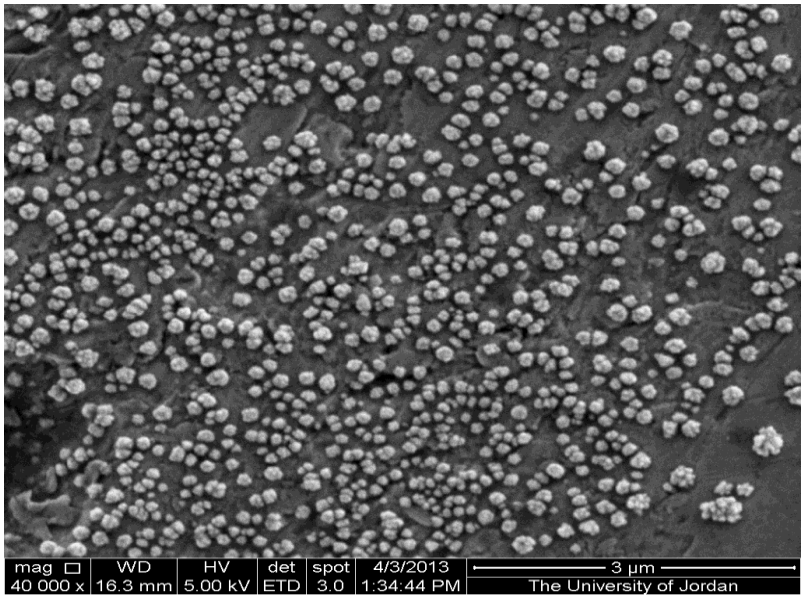

Figure 1. SEM micrograph of deposited platinum nanostructured surface on a tantalum substrate. Deposition experiment parameters: Square wave parameters : E_L = -0.4, E_H = 0 V, amplitude = 0.4V, frequency =100 Hz, $PtCl_6^-$ concentration= $1x10^{-4}$M, deposition time =120 seconds.

Figure 1 shows a representative SEM micrograph of an electrodeposited platinum nanostructured surface from $1.0x10^{-4}$ M $PtCl_6^-$ solution by application of a square wave potential regime.

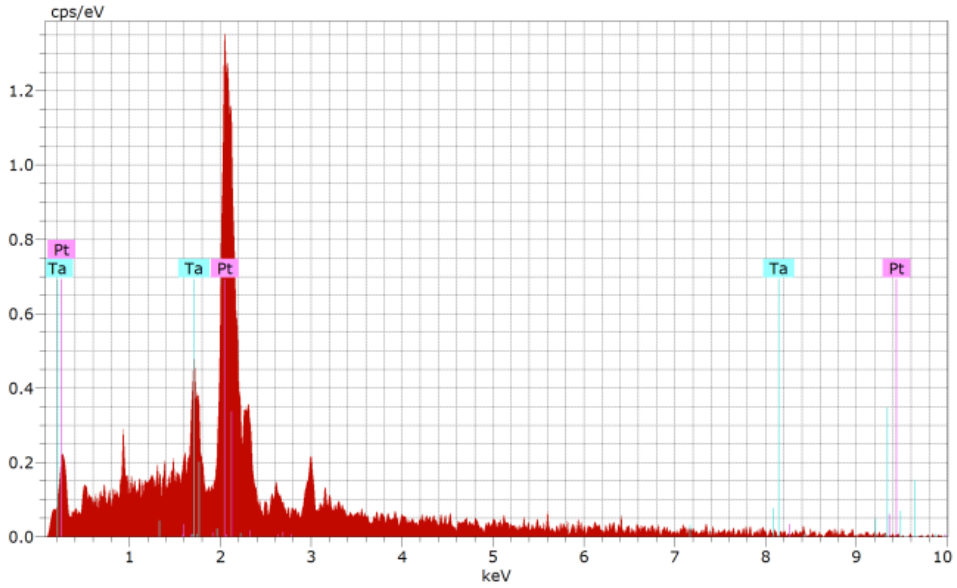

Figure 2. EDX spectra of deposited platinum nanostructure on tantalum electrode. Experimental parameters: E_L = -0.4, E_H = 0 V, amplitude = 0.4V, frequency =100 Hz, concentration= $1x10^{-4}$M, time = 120 seconds and scan rate = 100 mV/s.

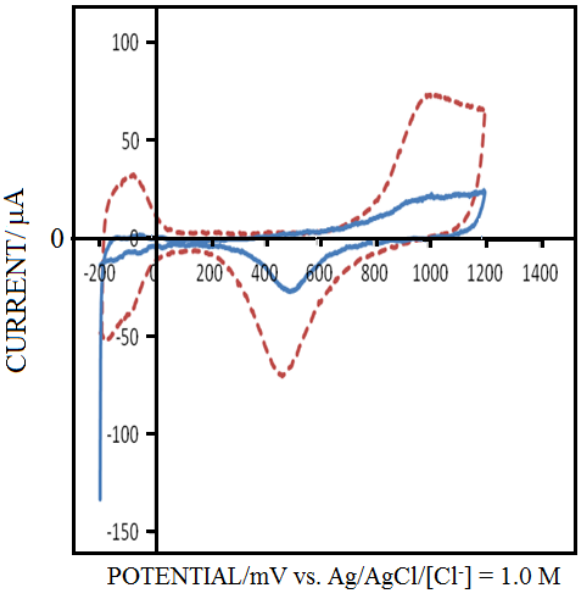

Figure 3. (—)Cyclic voltammogram of deposited platinum nanostructure on tantalum electrode in 0.5 M H_2SO_4 at a scan rate of 100 mV/s. Deposition experimental parameters: E_L = -0.4, E_H = 0 V, amplitude = 0.4V, frequency =100 Hz, deposition solution: 0.5 M H_2SO_4 + $1x0^{-4}$ M $PtCl_4^-$ deposition time =120 seconds. (-----) Cyclic voltammogram for polycrystalline platinum electrode with a different surface area under the same experimental conditions. .

The identity of the deposited particles was proved by energy-dispersive X- spectroscopy (Figure 2) and cyclic voltammetry (Figure 3). The EDX spectrum unequivocally confirms the identity of the deposited platinum nanostructures. The cyclic voltammogram for the nanostructured platinum electrode (Figure 3: the solid line) shows a great similarity to the voltammogram of the polycrystalline electrode (Figure 3: the dashed line) recorded under the same conditions. The three distinctive voltammetric features , the oxygen adsorption/desorption region, the hydrogen adsorption/ desorption region and the double layer region of platinum electrode are displayed on the voltammogram of the nanostructured electrode and the voltammogram for the polycrystalline electrode. Thus, through the high similarity between the cyclic voltammograms displayed by the two electrodes and the appearance of the well-known distinct voltammetric features of platinum electrodes, the identity of the nanostructured electrode is confirmed. Thus, the SEM micrographs along with the EDX spectra at one hand and the cyclic voltammetry on the other hand, prove the applicability of the square wave potential regime for preparation of platinum nanostructures. This result reinforces the results of our earlier work on preparation of gold, silver, and copper nanostructured surfaces by electrodeposition from their corresponding solutions by application of square wave potential regimes [12,13].

A rough estimate of the number of particles was calculated from the SEM micrographs. Table 1 shows the estimated number of particles as a function of $PtCl_6^-$ concentration in the supporting electrolyte in addition to some observations about the size of the particles and the uniformity of their distribution on the surface.

Table 1. The number of nanoparticles as a function of the concentration of $PtCl_6^-$ in the solution. Square wave parameters: frequency = 100 Hz, amplitude = 0.4 V, E_l= -0.4 V . E_h = 0.00 V.

No.	$[PtCl_6^-]$/mol L^- 1	Average /cm^2	Distribution uniformity	Particle Size
1	$1.0x10^{-3}$	$2x10^{14}$	Poor	3-dimensional
2	$5.0x10^{-4}$	$3.1x10^{14}$	Poor	Large
3	$1.0x10^{-4}$	$3.9x10^{14}$	Good	Small

The results of variation of deposition time are shown in Figure 4. The results of calculation of the number of particles are summarized in Table 2.

Table 2. The number of deposited nanoparticles as a function of the time of application of the square wave potential regime. Platimum particles were deposited from $1.0x10^{-4}$ M $PtCl_6^-$ solution. Square wave parameters: frequency = 100 Hz, amplitude = 0.4 V, E_l= 0.4 V . E_h = 0.00 V.

no.	**Deposition time (s)**	Average number of nanoparticles/cm^2	Distribution uniformity	Particle Size
1	90	-	Few Randomly	nanoparticles
2	120	$5.2 x10^{12}$	No uniform	nanoparticles
3	180	$4.1 x10^{12}$	-	3-d structures

From these results it can be concluded that increasing the time of deposition increases the density of the particles on the surface and the particle size too. Furthermore, larger concentrations and or longer deposition time lead to formation of 3-dimensional structures (Figure 4-C).

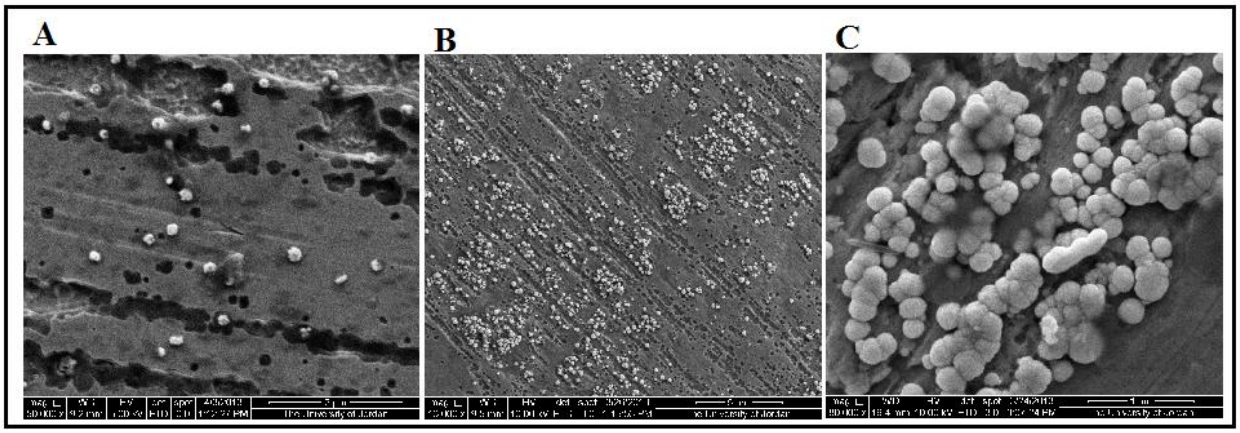

Figure 4. SEM micrograph of deposited platinum nanostructure on tantalum electrode at a variable time of deposition (A) 90 s (B) 120 s and (C) 180 s. Deposition experimental square wave parameters: E_L = -0.4, E_H = 0V, amplitude = 0.4V, frequency =100 Hz. Solution: 0.5 M H_2SO_4 + 1x10^{-4} M $PtCl_4^-$.

These results can be explained on basis of two competing mechanisms for platinum deposition on the tantalum substrate, namely nucleation and particle growth [14]. The results of this work strongly supports that particle growth is the prevailing mechanism of metal deposition at high concentrations and long deposition times. The initial stages of deposition involve nucleation, which occurs selectively at high-energy surface sites. These high-energy surface sites include surface defects, voids, adatoms, or grain boundaries. At low ion concentration, nucleation prevails because of the availability of high-energy surface sites. On the other hand, at high concentration of depositing ions, high surface energy sites are relatively limited thus making particle growth mechanism prevalent. On the same basis, the effect of deposition time can be explained. At short deposition times, nucleation mechanism prevails because of the availability of high-energy surface sites, while particle growth prevails when most of these sites are consumed at long deposition times. This would necessarily enhance the formation of 3-dimentional structures, at long deposition times

3.2. The effect of square wave frequency

Table 2 summarizes the effect of square wave frequency on the deposited platinum structures. These results indicate that 100 Hz is the optimal frequency for square-wave-deposition frequency. This result coincides with our earlier work on deposition of other metals where we found also that the best deposited particles were produced at similar frequencies [12,13] . This can be explained on basis that 100 Hz represents an intermediate frequency which allows a break even between the two deposition competing mechanisms, nucleation and particle growth. Moreover, at high frequencies the electrochemical system is taxed by IR potential drop and possible kinetic limitations.

3.3 Bismuth adatoms on Platinum nanoparticles

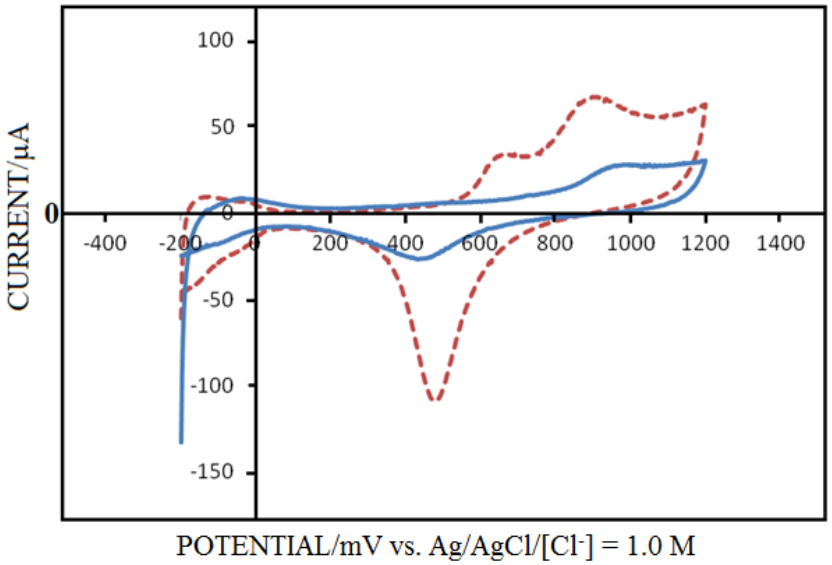

Figure 5. Cyclic voltammogram of platinum nanostructured electrode modified by bismuth adatoms (------ red) and the voltammogram of platinum nanostructured electrode (—blue) recorded in 0.5 M H_2SO_4 at a scan rate of 100 mV/s. Deposition square wave experimental parameters: E_L = -0.4, E_H = 0 V, amplitude = 0.4V, frequency =100 Hz. Deposition solution: concentration= $1x10^{-4}$M, time =120 s.

Figure 5 shows a representative cyclic voltammogram of a platinum nanostaructured electrode with adsorbed bismuth adatoms (given the symbol $Pt_{nano}Bi_{ad}$) along with the voltammogram of nanostructured platinum surface (Pt_{nano}) deposited on tantalum electrode. The voltammogram shows a peak centered at 0.66 V which is easily assignable to the irreversibly adsorbed bismuth atoms. Though the voltammogram (Figure 5) was recorded in a bismuth-free supporting electrolyte solution, scan rate-peak current functionality was furtherly tested. The experimentally determined relationship for the peak current assigned to Bi adatom oxidation was, $i_p \alpha \nu$ (R^2=0.998) where i_p is the bismuth oxidation peak current and ν is the scan rate. This result provides a conclusive evidence that these peaks are associated with a surface process rather than a bulk process. Further evidence for irreversible adsorption of bismuth at nanostructured platinum surfaces is shown in Figure 6. The EDX spectrum shows two peaks for bismuth adsorbed along with platinum and tantalum peaks.

The stability of bismuth adatoms on platinum nanostructured surfaces was traced by cyclic voltammetry. The consistency of the area under oxidation peak by time was taken as a criterion for the stability of bismuth adatom on platinum nanostructures. The peaks assigned to adsorption of bismuth atoms were still observed one week after preparation of these surfaces though there is a little decay in the peak height. The decay in peak current is attributed to desorption of Bi atoms from the surface upon scanning in the oxidation region.

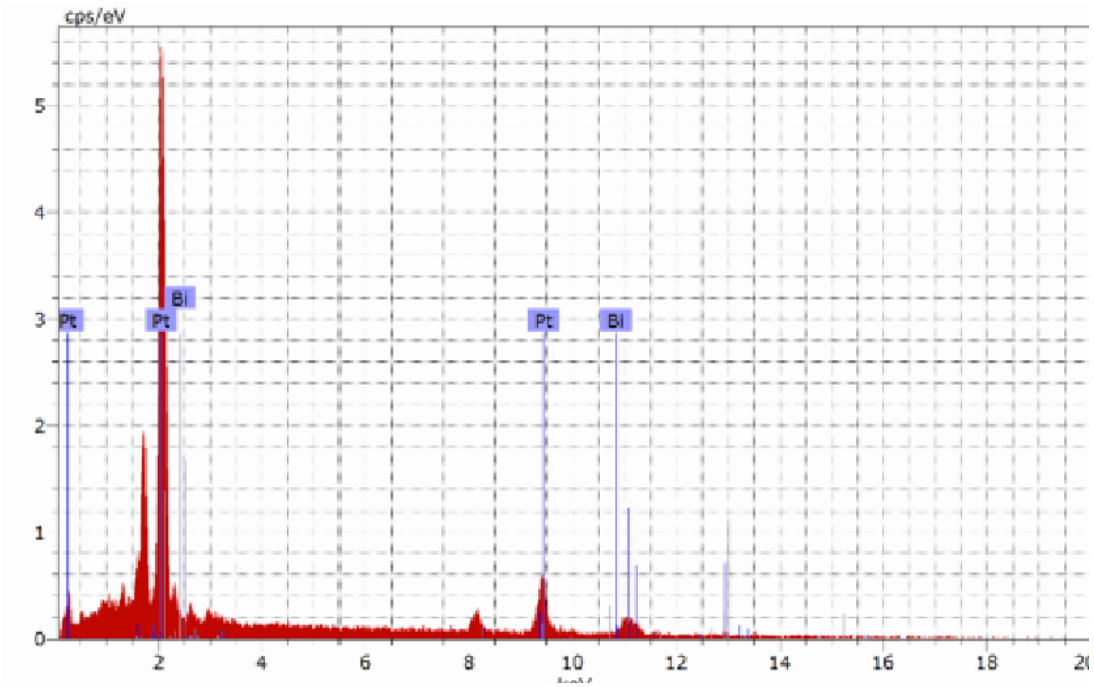

Figure 6. EDX spectra of deposited platinum nanostructures on a tantalum substrate modified with bismuth adatoms. Deposition experimental parameters of the square wave: E_L = -0.4, E_H = 0 V, amplitude = 0.4V, frequency =100 Hz. Solution: 0.5 M H_2SO_4 + 1x10^{-4} M $PtCl_4^-$, deposition time= 120 seconds. Modification with Bi adatoms was carried out by exposure of the platinum nanostructured electrode to 0.5 M H_2SO_4 1x10^{-2} M Bi^{3+} solution at open circuit for 5 min.

From the voltammograms of nanostructured platinum electrode and the voltammogram of nanostructured platinum electrode modified with Bi atoms, the areas under hydrogen desorption peak in presence and in absence of Bi atoms were integrated. From these areas the coverage of Bi adatoms at the surface was determined to be 0.66. Thus about two thirds of a monolayer of Bi is irreversibly adsorbed at the surface. The details of the method of calculation of the coverage of adatoms at platinum surfaces is published in one of our earlier publications [15]. This result is not unexpected because platinum is well known to irreversibly adsorb bismuth atoms (8,10).

3.4 Oxidation of small organic molecules at $Pt_{nano}Bi_{ad}$ electrodes

Figure 7 shows the voltammograms of $Pt_{nano}Bi_{ad}$ electrode in 0.5 M H_2SO_4 + 0.010 M CH_3OH along with the voltammogram of Pt_{nano} electrode under the same experimental conditions. The voltammogram for $Pt_{nano}Bi_{ad}$ electrode shows a huge increase in the charge attributed to oxidation of methanol compared to the charge for oxidation of methanol at the nonostructured platinum electrode. The whole oxidation region starting from nearly 0.1 V to 1.2 V is dominated by the oxidation features of methanol. Oxidation of methanol merges with the surface oxidation as manifested by the appearance of oxygen desorption cathodic peak centered at 0.4 V. The voltammetric features for electrooxidation are manifested by three peaks centered at 0.40 V, 0.69 V and 0.95 V. The appearance of a large charge for electrooxidation of methanol is a manifestation of the high electrocatalytic

properties of the Pt_{nano}-Bi_{ad} electrode. Furthermore, the threshold of methanol electrooxidation is about +0.1 V Pt_{nano}-Bi_{ad} compared to a value of +0.30 V at Pt_{nano} electrode. This amounts to a 200 mV potential advantage at the adatom nanostrucured electrode which also indicates higher catalytic properties for the Pt_{nano}-Bi_{ad} electrode.

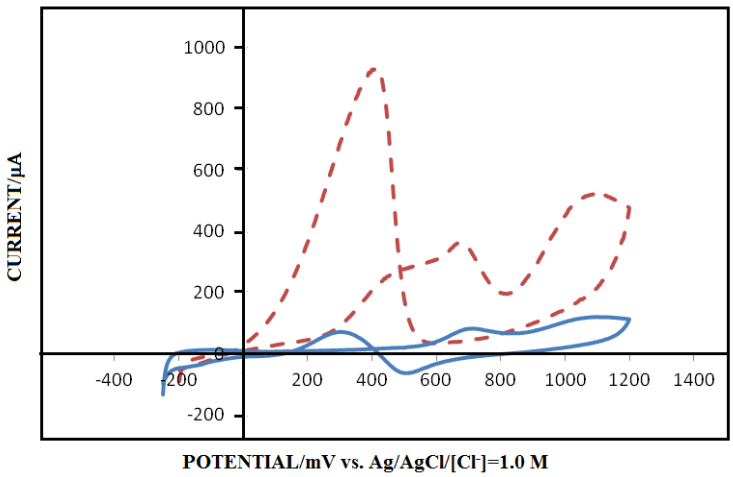

Figure 7. Cyclic voltammograms of nanostructured platinum electrode modified by bismuth adatoms (---- red) and platinum nanostructured electrode (—— blue) recorded in 0.5 M H_2SO_4 + $1x10^{-2}$ M methanol at a scan rate of 100 mV/s. Experimental parameters for platinum deposition: E_L = -0.4, E_H = 0 V, amplitude = 0.4V, frequency =100 Hz, concentration= $1x10^{-4}$M $PtCl_4^-$, deposition time = 120 seconds.

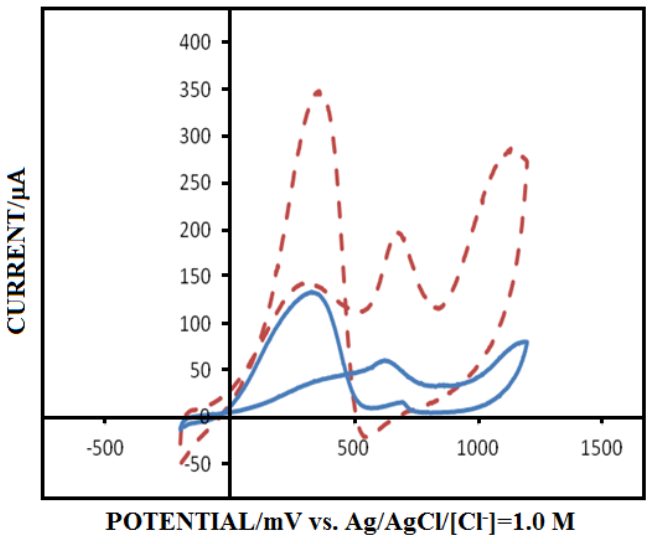

Figure 8. Cyclic voltammograms of nanostructured platinum electrode modified by bismuth adatoms (----- red) and platinum nanostructured electrode (—— blue) recorded in 0.5 M H_2SO_4 + $1x10^{-2}$ M HCOOH at a scan rate of 100 mV/s. Experimental parameters for platinum deposition: E_L = -0.4, E_H = 0 V, amplitude = 0.4V, frequency =100 Hz, concentration= $1x10^{-4}$M $PtCl_4^-$, deposition time = 120 seconds.

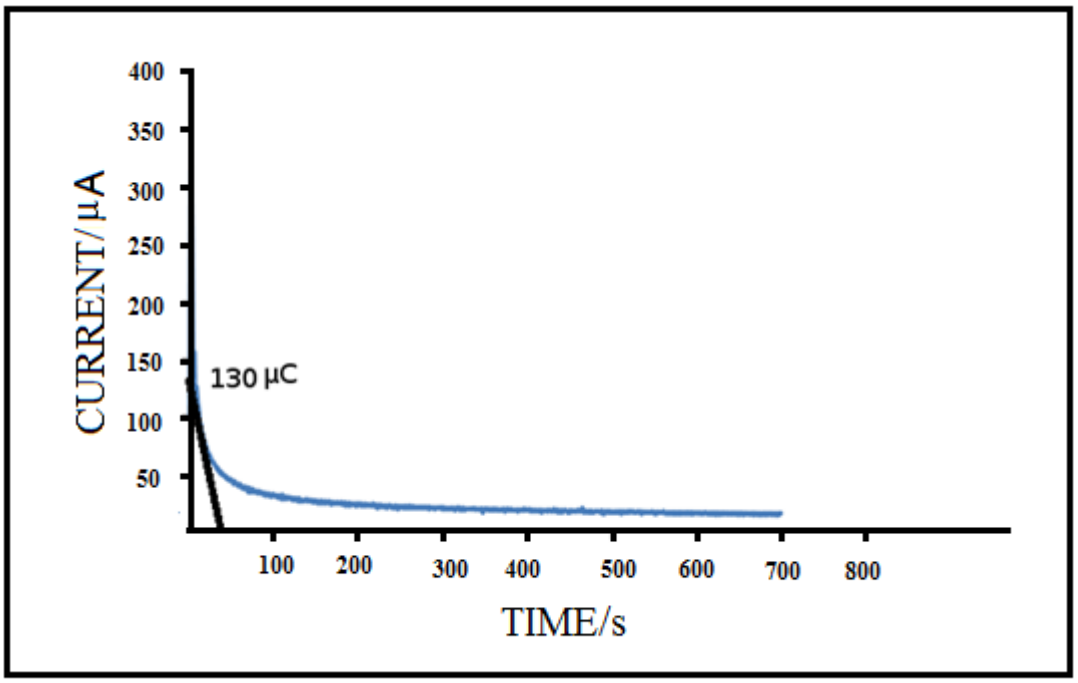

Figure 9. Chronoamperogram (current-time profile) for a platinum nanostructured electrode dosed with 0.66 monolayer of Bi adatoms ($Pt_{nano}Bi_{ad}$) electrode 0.5 M H_2SO_4+1x10^{-3} M HCOOH. Experiment parameters are : Initial potential = 0.15 V , Final potential = 0.80 V , time = 700 ms.

Figure 8 shows the voltammograms of Pt_{nano}-Bi_{ad} electrode in 0.5 M H_2SO_4 + 0.01 M HCOOH along with the voltammogram of Pt_{nano} electrode in the same solution. Oxidation of formic acid shows a large increase in the oxidation charge of formic acid compared to oxidation of formic acid before modification with bismuth adatoms. This finding is indicative of enhanced electrocatalytic properties of the platinum nanoparticles by adsorption of bismuth adatoms.

The chronoamperometric current profile for a potential step experiment from 0.15 V to 0.8 V region is displayed in Figure 9. The kinetically controlled current was measured from the i-t current profile, the real surface area from the voltammogram was calculated as 0.31 cm^2. The rate constant for the forward reaction for oxidation of formic acid was calculated according to equation 1[16]

$k_f = i_k/nFAC^*$ …….1

Where k_f is the kinetically controlled reaction rate constant, n is the no. of electrons transferred in the process, A is the surface area of the electrode, F faraday's constant and C* is the bulk concentration of formic acid. Upon application of equation 1, the calculated k_f value is 0.44 compared to a value of 0.081 for Pt_{nano} electrode under the same experimental conditions which provides another experimental evidence for the enhanced electrocatalytic activities of the $Pt_{nano}Bi_{ad}$ electrode by a factor of 5.4. Electrocatalysis of formic acid oxidation by bismuth adatoms has been attributed to the positive charge developed at Bi atoms adsorbed at the surface of platinum. The positive charge acquired by Bi adatoms adsobs the formate anion which assists in breakage of H-C bond by the neighboring Pt atoms[17]. Electrocatalysis produced at nanostructured electrodes has been reported too as a result of low index planes displayed by nanostructured surfaces[1]. The combination of the electrocatalytic

synergism has not been published before. The present work has shown that the effects of the two factors are additive rather than competitive.

4. CONCLUSIONS

The present work proved the applicability of square wave potential regime to preparation of nanostructured platinum electrodes. This result conforms with our previous results on preparation of gold, silver and copper nanoparticles by application of square potential regimes. Similarly, the size, uniformity of distribution and shape of the particles were found to be dependent on the square wave parameters namely, the frequency, amplitude, and higher and lower limits of the square wave in addition to the concentration of the ions of metal in the solution and the time of application of the square wave.

Synergistic electrocatalytic effects of underpotentially irreversibly adsorbed atoms on the prepared platinum nanostructures has been proved by investigation of electrooxidation of methanol and formic acid at Pt_{nano}-Bi_{ad} electrodes. For both test molecules, an enhanced oxidation charge was observed for the Bi-modified nanostructured platinum electrode. This attests to the enhanced electrocatalytic properties of the modified electrode imparted by adatoms.

References

1. R. Murray, *Chem. Rev*., 108 (2008) 2688.
2. M. Hunglemann, P. Hunglemann, W. J. Lorenz, W. Schnider, *Surface science*, 597 (2005) 156.
3. N. M. Markovic, P. N. Ross, *Surface Science Reports*, 45 (2002) 121.
4. A. N. Shipway, E. Katz, I. Willner, *Chem. Phys. Chem.*, 1(2000).
5. M. El-Deab, T. Osaka, *J. Electroanal. Chem.*, 553(2003) 107.
6. U. S. Mohanty, *J. Applied Electrochem*. 41(2011) 257.
7. D. P. Woodfuff (Ed), *The Chemical Physics of Solid Surfaces*, 2002, Elsevier, Amsterdam.
8. J. Clavilier, A. Fernandez-Viga, J. M. Feliu, A. Aldaz, *J. Electroanal. Chem*, 258 (1989) 89.
9. S. Sun, S. Chen, S. Li, N. Lu, G. Chen, F. Xu, *Colloids and Surfaces, A: Physicochemical and Engineering Aspects*, 134 (1998) 207.
10. S. Motoo, M. Watanabe, *J. Electroanal. Chem.*, 98 (1997) 203.
11. A. S. Cambell, R. Parsons, *J. Chem. Soc. Faraday Trans*, 88 (1992) 833.
12. M. K. Hourani, W. Mahmood, AFINDAD, 71 (2014) 299.
13. M. K. Hourani, T. Hamdan, *Surface Engineering and Applied Electrochemistry*, 49 (2013) 247.
14. S. C. S. Lai, A. Robert, R. A. Lazenby, P. M. Kirkman., P. R. Unwin, *Chem. Sci.* 6 (2015) 1126.
15. W. Qaddumi, M. Hourani, *Analytical Chemistry: An Indian Journal*, 12(11) (2013) 403.
16. A. Bard, F. Faulkner, *Electrochemical Methods: Fundamentals and Applications* (2nd ed). (2001) New York: Wiley and sons.
17. A. Ferre-Vilaplana, J. V. Perales-Rondon, J. M. Felu, E. Herrero, *ACS Catalysis*, 5(2), (2015), 645.